The rotational spectrum of the CD_2 radical studied by far infrared laser magnetic resonance spectroscopy[a)]

P. R. Bunker, Trevor J. Sears, and A. R. W. McKellar

Herzberg Institute of Astrophysics, National Research Council of Canada, Ottawa, Ontario, Canada K1A OR6

K. M. Evenson

National Bureau of Standards, Boulder, Colorado 80303

F. J. Lovas

National Bureau of Standards, Washington, D.C. 20234
(Received 7 March 1983; accepted 22 April 1983)

We report the detection of 17 pure rotation transitions in the ground vibronic state of the CD_2 radical using far infrared laser magnetic resonance spectroscopy. Fitting the data using an effective rotational Hamiltonian yields values for the three rotational constants, seven centrifugal distortion constants, the three electronic spin-rotation, and two electronic spin–spin parameters. We also fit this data, and CD_2 ν_2 band data (published separately), using the semirigid bender Hamiltonian and obtain the effective bending potential function for CD_2. Combining this with previous CH_2 results enables us to predict the rotation bending energy levels of CHD. We also report here the detection of two further rotational transitions in the ν_1 excited vibrational state of CH_2.

I. INTRODUCTION

Recently, high resolution infrared laser magnetic resonance spectra of gas phase CH_2 in its ground $\tilde{X}^3B_1$ state have been obtained.[1–3] Analysis of these data has yielded, among other things, values for the equilibrium geometry and the height of the barrier to linearity.[4] The fine and hyperfine splitting parameters have also been determined for the ground vibronic state[2] and fine structure parameters for the ν_2 (bending) excited state.[3] It was possible, using this data, to make predictions[4] of the spectra of CD_2 and $^{13}CH_2$. These predictions facilitated LMR measurements of the ν_2 band of $^{13}CH_2$ which were subsequently made.[5] The present paper reports the detection and assignment of the far infrared LMR spectrum of CD_2, and in the following accompanying paper[6] the diode laser spectrum of part of the ν_2 band of CD_2 is reported.

In this paper we report the detection of 17 pure rotation transitions in the ground state of CD_2 and we analyze them using both the effective rotational Hamiltonian and (with the inclusion of the ν_2 band data[6]) the semirigid bender Hamiltonian, as was done for CH_2 in Refs. 2 and 3. Comparison of the parameters obtained here for CD_2 with those obtained previously for CH_2 is of interest, and enables us to predict the rotation-bending energy levels of CHD. We also report here the detection of two more rotational transitions in the ν_1 excited vibrational state of CH_2. The data obtained here, and in Ref. 6, augment those obtained previously for CH_2[1–3] and $^{13}CH_2$[5] and, in another accompanying paper,[7] all this rotation-vibration data is fitted using the nonrigid bender Hamiltonian to provide an $\tilde{X}^3B_1$ potential surface that is a refinement of that determined before[4] in which only CH_2 data was used.

[a)]Work supported in part by NASA contract W-15047.

II. EXPERIMENTAL DETAILS AND RESULTS

All the spectra were recorded at the NBS Boulder Laboratory using the far infrared LMR spectrometer described previously.[2] The CD_2 radicals were produced in the far infrared cavity by a flowing reaction between perdeuterated methane and fluorine atoms; the fluorine atoms were produced by flowing F_2 in helium through a microwave discharge. Optimum signal strength was obtained with partial pressures of 50 Pa He, 1 Pa F_2, and 0.5 Pa CD_4 (where 1 Pa ≃ 7.5 mTorr).

Before beginning the search the frequencies of appropriate CD_2 rotational transitions were calculated using the CD_2 term values predicted by Jensen, Bunker, and Hoy.[4] These predictions were made using the potential surface obtained by fitting the eigenvalues of the nonrigid bender Hamiltonian to the experimentally measured[2,3] rotation and rotation-vibration intervals for CH_2. Using far infrared laser lines close to these predicted frequencies strong spectra were detected, and these were assigned to CD_2 with some confidence on the basis of their closeness to the theoretical predictions, the chemistry of their production, and on their nuclear hyperfine structure (when present). Subsequent detailed analysis, reported below, confirmed the assignment.

Examples of spectra recorded using the 107.5 μm CD_3OD laser line are shown in Figs. 1–3. The spectrum shown in Fig. 1 was obtained with the electric vector of the laser radiation parallel to the magnetic field direction (i.e., in π polarization), and that shown in Fig. 2 with it perpendicular to it (σ polarization). In Fig. 3 a scan through a strong resonance at 0.3401 T in π polarization is shown; the magnetic field modulation amplitude and sample pressure were both reduced to obtain this spectrum. The resonances in Figs. 1–3

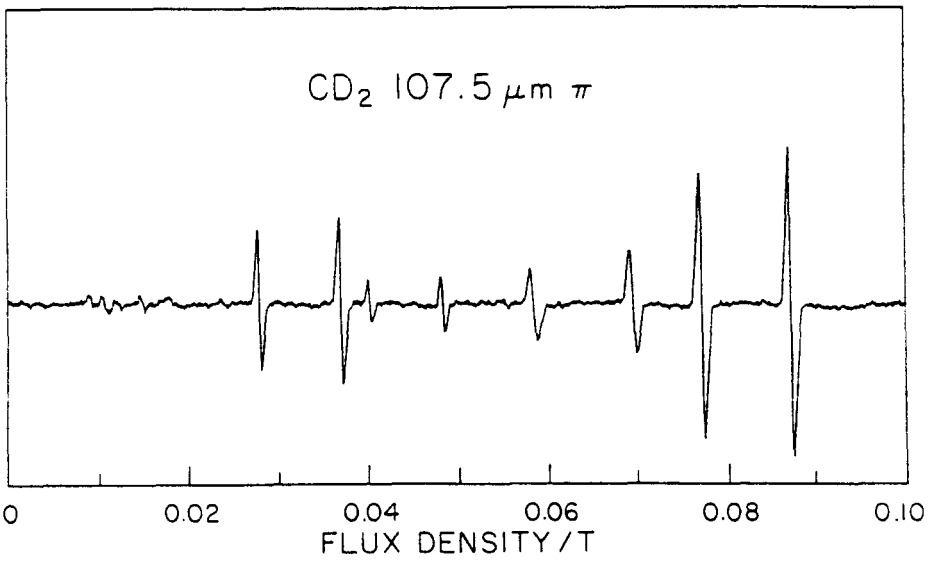

FIG. 1. Laser magnetic resonance spectrum of CD_2 obtained with the 107.5 μm (92.9906 cm^{-1}) laser line of CD_3OD in parallel polarization. These resonances are various Zeeman components of the $3_{21} - 3_{12}$ rotational transition (see Table II).

are assigned as components of the $3_{21} - 3_{12}$ rotational transition, and the saturation features (inverse Lamb dips) show the expected quintet and singlet hyperfine structure. For most of our spectra the nuclear hyperfine structure was not well resolved.

In all nearly 200 resonances were assigned to components of 17 rotational transitions. The laser lines used are given in Table I and a complete list of the resonances is given in Table II. The assignments were made, with the help of the nonrigid bender predictions,[4] using a desktop calculator and plotter to draw Zeeman spectrum plots as described previously.[1-3]

III. ANALYSIS OF RESULTS

A. Using the effective rotational Hamiltonian

The effective rotational Hamiltonian for a vibrational level of the $^3B_1$ state of CH_2 was discussed in Ref. 2, and we use the same Hamiltonian for CD_2. We have not attempted to analyze the fragmentary and poorly resolved nuclear hyperfine structure. The Hamiltonian involves rigid rotor, centrifugal distortion, electronic spin–spin interaction, electronic spin-rotation interaction, and Zeeman effect terms as given, respectively, in Eqs. (2), (3), (4), (5), and (7) of Ref. 2.

The computer program[2] used in the fitting was based on that described by Barnes *et al.*[18] and it sets up the matrix of the Hamiltonian operator in a fully coupled prolate symmetric top basis set which is truncated at a point empirically found to cause negligible change in the eigenvalues of interest. In the present case the basis set included all states up to and including matrix elements with $\Delta N = \pm 2$ and $\Delta K = \pm 2$. In the fit of the eigenvalues of this Hamiltonian matrix to our data we adjusted 15 parameters; the refined values of these parameters, and their standard errors, are given in Table III. The standard deviation of the fit is 5.2 MHz and the (observed-calculated) values for all the assigned

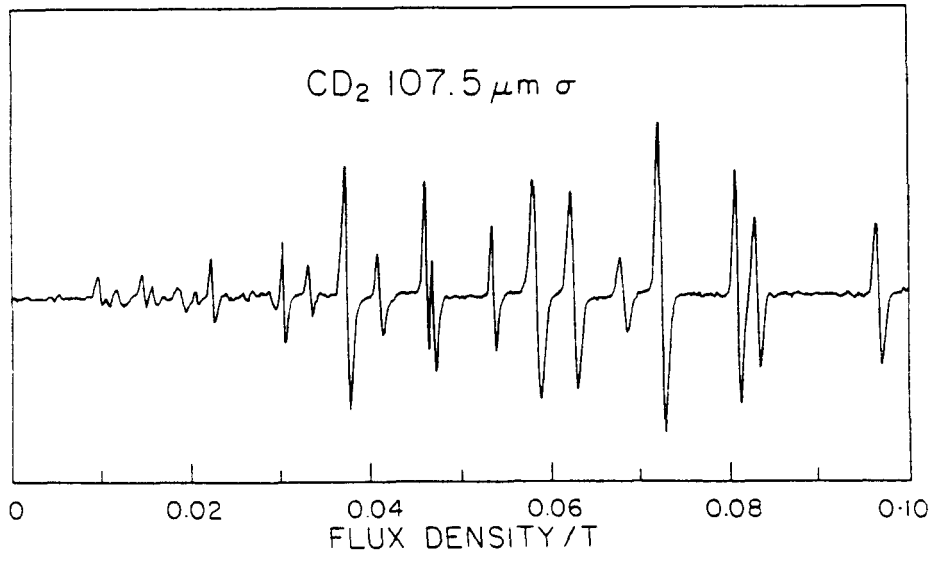

FIG. 2. Same as in Fig. 1, but with perpendicular polarization of the laser radiation relative to the Zeeman field.

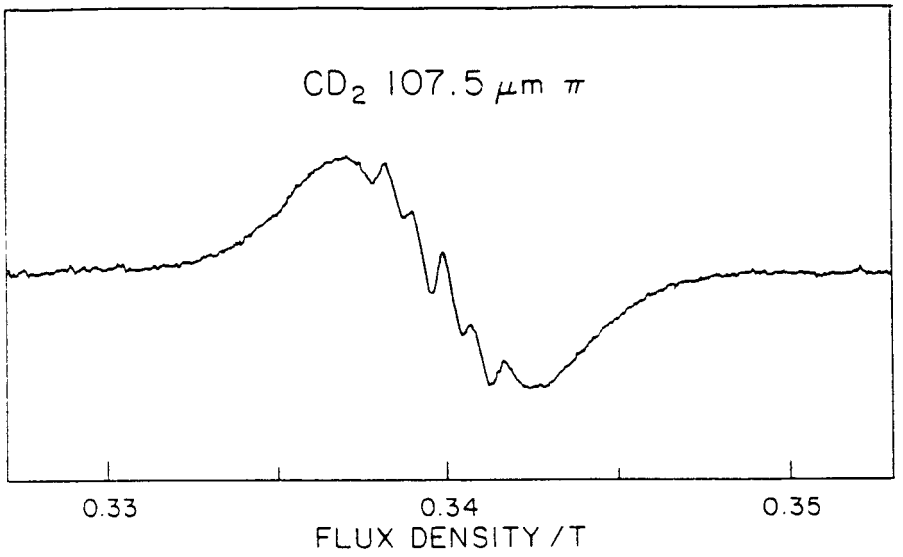

FIG. 3. One Zeeman component of the $3_{21} - 3_{12}$ rotational transition of CD_2, showing saturation dips due to partially resolved hyperfine structure.

TABLE I. Far infrared laser lines used to observe LMR spectra of CD_2.

Lasing gas	Laser wavelength (μm)	Laser wave number (cm^{-1})	CD_2 transitions
CH_3OH	570.6	17.526 375[a]	$1_{11} - 2_{02}$
CD_3OD	298.7	33.474 377[b]	$2_{11} - 2_{02}$, $1_{10} - 1_{01}$
CH_2F_2	287.7	34.762 374[c]	$2_{11} - 2_{02}$; $3_{12} - 3_{03}$
CD_2F_2	248.1	40.305 013[d]	$1_{11} - 0_{00}$
CH_2OH	242.5	41.241 758[e]	$1_{11} - 0_{00}$
CH_2DOH	206.7	48.382 240[f]	$2_{12} - 1_{01}$
CD_2OH	180.7	55.327 940[g]	$3_{13} - 2_{02}$
CH_3OH	170.6	58.624 765[a]	$4_{22} - 5_{15}$
CH_2F_2	166.6	60.012 827[c]	$3_{22} - 4_{13}$
CD_3OH	144.1	69.387 647[g]	$2_{21} - 3_{12}$; $5_{15} - 4_{04}$
CH_2DOH	108.8	91.896 764[f]	$4_{22} - 4_{13}$
CD_3OD	107.5	92.990 646[b]	$2_{20} - 2_{11}$; $3_{21} - 3_{12}$
$^{13}CH_3OH$	103.5	96.636 268[h]	$3_{22} - 3_{13}$; $4_{23} - 4_{14}$
$^{13}CH_3OH$	85.3	117.209 532[h]	$3_{22} - 2_{11}$

[a] F. R. Petersen, K. M. Evenson, D. A. Jennings, J. S. Wells, K. Goto, and J. J. Jimenez, IEEE J. Quant. Electron. 11, 838 (1975).
[b] E. C. C. Vasconcellos, A. Scalabrin, F. R. Petersen, and K. M. Evenson, Int. J. IR Mm Waves 2, 533 (1981).
[c] F. R. Petersen, A. Scalabrin, and K. M. Evenson, Int. J. IR Mm Waves 1, 111 (1980).
[d] E. C. C. Vasconcellos, F. R. Petersen, and K. M. Evenson, Int. J. IR Mm Waves 2, 705 (1981).
[e] F. R. Petersen, K. M. Evenson, D. A. Jennings, and A. Scalabrin, IEEE J. Quant. Electron. 16, 319 (1980).
[f] A. Scalabrin, F. R. Petersen, K. M. Evenson, and D. A. Jennings, Int. J. IR Mm Waves 1, 117 (1980).
[g] R. J. Saykally, K. M. Evenson, D. A. Jennings, and F. R. Petersen (in preparation).
[h] J. O. Henningsen, J. C. Petersen, F. R. Petersen, D. A. Jennings, and K. M. Evenson, J. Mol. Spectrosc. 77, 298 (1979).

resonances are included in Table II. The electron spin g factors were fixed at the values predicted by Curl's relation[9] and the (small) rotational g factors at values predicted from simple theory.[8]

In the fit all the varied parameters are well determined and the only off-diagonal correlation coefficient greater than 0.9 is that between $\frac{1}{2}(B-C)$ and δ_K which was 0.9953. As with the fit[2] for CH_2 a large number of centrifugal distortion parameters are necessary because of the bending flexibility in this molecule, but the problem is less severe in CD_2 than in CH_2 because the (000) vibrational level is lower in the potential well. Also as for CH_2 we could not assign any resonances involving transitions to levels with $K_a > 2$ and, therefore, we could not determine Φ_K. This parameter was fixed at a value obtained from a fit using the nonrigid bender Hamiltonian.[7]

In the effective Hamiltonian fits[2,3] for CH_2 there was no need to include centrifugal distortion corrections to the spin–spin and spin-rotation interactions, and this is equally true for CD_2. For the vibronic ground state the values obtained for D and E, the dominant fine structure parameters, are compared with those obtained for CH_2 and $^{13}CH_2$ in Table IV, and we see that D is smaller in CD_2 than in CH_2, whereas E is larger. The increase in E can be understood since CD_2 is somewhat more bent in the (000) state than CH_2 and E is zero for a linear molecule. The spin-rotation parameters ϵ_{aa}, ϵ_{bb}, and ϵ_{cc} are all well determined although they make a much smaller contribution to the observed fine structure splittings. When compared to their values for CH_2 it is evident that they scale as the corresponding rotational constants, as might be expected from simple theoretical arguments.

We tried extensively to find transitions involving $K_a = 3$ energy levels, but without success. The number of available far infrared laser lines is very limited for frequencies greater than 100 cm^{-1} where most CD_2 transitions involving levels with $K_a \geq 3$ occur, and this

TABLE II. Observed resonant fields of LMR transitions in the ground state of CD_2.

Laser line (cm^{-1})[a]	Resonant field (T)[c]	Assignment[b]			Obs.–Calc.			
		$N_{K_aK_c}$	J	M_J	(MHz)	(G)[c]	TR[d]	Int[e]
17.5267	0.34570	1 1 1—2 0 2	2—3	1— 1	−0.1	0.0	2.72	2
17.5267	0.41810	1 1 1—2 0 2	2—3	2— 2	−4.5	2.0	2.31	1
17.5267	0.42550	1 1 1—2 0 2	2—1	−1—−1	−0.9	0.4	2.41	1
17.5267	0.38050	1 1 1—2 0 2	2—3	−1—−2	−4.9	2.0	2.47	3
17.5267	0.49110	1 1 1—2 0 2	2—3	1— 2	−1.5	0.6	2.36	2
33.4744	0.22991	2 1 1—2 0 2	1—2	1— 1	−8.3	−1.8	−4.64	47
33.4744	0.27011	2 1 1—2 0 2	1—2	0— 0	−6.6	−1.4	−4.72	39
33.4744	0.64174	2 1 1—2 0 2	3—2	2— 2	−5.6	−2.2	−2.52	31
33.4744	0.04124	1 1 0—1 0 1	1—2	1— 0	0.0	0.0	1.33	81
33.4744	0.04533	1 1 0—1 0 1	1—2	−1—−2	−0.1	0.1	1.09	295
33.4744	0.05259	1 1 0—1 0 1	1—2	0—−1	0.0	0.0	0.76	208
33.4744	0.34687	1 1 0—1 0 1	2—1	0—−1	−2.0	2.6	0.76	371
33.4744	0.83341	1 1 0—1 0 1	2—1	1— 0	−0.9	5.2	0.17	464
34.7624	0.29956	2 1 1—2 0 2	2—1	0— 0	7.2	−1.6	4.54	37
34.7624	0.36195	2 1 1—2 0 2	2—1	−1—−1	5.1	−1.0	5.02	48
34.7624	0.59740	2 1 1—2 0 2	2—3	−1—−1	7.9	−3.1	2.56	30
34.7624	0.62787	2 1 1—2 0 2	2—3	−2—−2	4.9	−1.9	2.64	18
34.7624	0.24255	2 1 1—2 0 2	2—1	2— 1	10.8	−2.3	4.68	46
34.7624	0.29325	2 1 1—2 0 2	2—1	1— 0	9.4	−2.1	4.51	40
34.7624	0.22359	3 1 2—3 0 3	2—4	1— 1	1.5	0.7	−2.23	9
34.7624	0.33057	3 1 2—3 0 3	2—4	0— 0	2.5	1.1	−2.38	3
34.7624	0.27027	3 1 2—3 0 3	3—3	−3—−2	21.5	12.5	−1.72	79
34.7624	0.27207	3 1 2—3 0 3	2—4	0— 1	1.1	0.5	−2.32	18
34.7624	0.27683	3 1 2—3 0 3	2—4	−1—−2	2.0	0.6	−3.26	16
34.7624	0.29695	3 1 2—3 0 3	4—3	4— 3	−8.2	8.3	0.98	152
34.7624	0.32655	3 1 2—3 0 3	2—4	−2—−1	4.3	1.6	−2.75	13
34.7624	0.33168	3 1 2—3 0 3	2—4	0—−1	2.2	0.8	−2.69	14
34.7624	0.34551	3 1 2—3 0 3	2—4	−1— 0	2.6	1.0	−2.46	44
34.7624	0.36712	3 1 2—3 0 3	4—4	3— 4	2.6	1.1	−2.42	33
40.3050	0.34197	1 1 1—0 0 0	1—1	0— 1	0.4	0.1	−5.37	49
41.2418	0.19270	1 1 1—0 0 0	0—1	0— 0	0.2	−0.1	1.75	240
41.2418	0.33976	1 1 1—0 0 0	2—1	−1—−1	3.6	−1.3	2.69	57
41.2418	0.05842	1 1 1—0 0 0	0—1	0—−1	0.1	0.0	3.40	346
41.2418	0.33977	1 1 1—0 0 0	2—1	1— 0	4.4	−1.6	2.69	58
48.3822	0.00340	2 1 2—1 0 1	3—2	−2—−2	−1.6	1.7	0.91	797
48.3822	0.00700	2 1 2—1 0 1	3—2	−1—−1	−1.6	3.7	0.43	1276
48.3822	0.17734	2 1 2—1 0 1	3—2	0— 0	−1.8	4.6	0.38	1409
48.3822	0.18278	2 1 2—1 0 1	2—1	−1—−1	−6.4	2.4	2.64	283
48.3822	0.80272	2 1 2—1 0 1	2—1	0— 0	−1.9	10.5	0.18	1154
48.3822	0.00140	2 1 2—1 0 1	3—2	−1—−2	3.8	−2.0	1.86	159
48.3822	0.00222	2 1 2—1 0 1	3—2	0—−1	−1.1	0.8	1.39	479
48.3822	0.00336	2 1 2—1 0 1	3—2	1— 0	−1.3	1.5	0.92	956
48.3822	0.00674	2 1 2—1 0 1	3—2	2— 1	−1.3	2.8	0.46	1594
48.3822	0.06803	2 1 2—1 0 1	1—2	−1—−2	−1.1	0.3	3.27	125
48.3822	0.15090	2 1 2—1 0 1	2—1	0—−1	−6.0	2.0	2.94	58
48.3822	0.18713	2 1 2—1 0 1	3—2	−1— 0	−1.3	1.2	1.07	503
48.3822	0.53480	2 1 2—1 0 1	3—2	2— 1	−0.6	−5.6	−0.10	2264
48.3822	0.60361	2 1 2—1 0 1	2—1	1— 0	−3.4	11.9	0.28	388
55.3279	0.36126	3 1 3—2 0 2	2—3	0— 0	−0.1	0.0	−2.19	35
55.3279	0.40162	3 1 3—2 0 2	4—3	3— 3	0.6	0.3	−2.33	198
55.3279	0.50971	3 1 3—2 0 2	4—2	−2—−2	−10.9	31.1	0.35	1087
55.3279	0.29380	3 1 3—2 0 2	2—3	1— 0	0.7	0.4	−1.97	25
55.3279	0.29822	3 1 3—2 0 2	4—3	2— 3	−0.1	0.0	−2.68	23
55.3279	0.36276	3 1 3—2 0 2	2—3	−2—−1	−0.2	−0.1	−2.90	6
55.3279	0.36343	3 1 3—2 0 2	2—3	0—−1	1.5	0.6	−2.79	28
55.3279	0.35523	3 1 3—2 0 2	2—3	−1— 0	0.1	0.0	−2.82	111
58.6248	0.02280	4 2 2—5 1 5	5—5	−5—−5	17.5	7.4	−2.23	1
58.6248	0.02540	4 2 2—5 1 5	5—5	−4—−4	−4.4	−2.1	−2.13	11
58.6248	0.03030	4 2 2—5 1 5	3—5	−3—−3	−4.0	−2.0	−1.96	8
58.6248	0.03619	4 2 2—5 1 5	3—5	−2—−2	−10.9	−5.9	−1.84	7
58.6248	0.04130	4 2 2—5 1 5	3—5	−1—−1	−2.7	−1.6	−1.72	7
58.6248	0.15971	4 2 2—5 1 5	5—5	−2—−2	0.2	0.1	−1.28	1
58.6248	0.27940	4 2 2—5 1 5	5—5	−3—−3	0.6	0.3	−1.60	1
58.6248	0.03410	4 2 2—5 1 5	3—5	−2—−1	−7.4	−3.9	−1.93	11
58.6248	0.07020	4 2 2—5 1 5	5—5	0— 1	−2.3	−2.2	−1.08	3

TABLE II (*Continued*)

Laser line $(cm^{-1})^a$	Resonant field (T)[c]	Assignment[b] $N_{K_aK_c}$	J	M_J	Obs.−Calc. (MHz)	(G)[c]	TR[d]	Int[e]
58.6248	0.10740	4 2 2 — 5 1 5	5 — 5	−1 — −2	0.6	0.7	−0.89	8
58.6248	0.13480	4 2 2 — 5 1 5	5 — 5	2 — 3	−3.4	−2.7	−1.25	28
58.6248	0.19330	4 2 2 — 5 1 5	5 — 5	−2 — −3	3.2	2.6	−1.25	22
58.6248	0.21110	4 2 2 — 5 1 5	5 — 5	3 — 4	−2.8	−2.1	−1.38	48
58.6248	0.34070	4 2 2 — 5 1 5	5 — 5	−3 — −4	1.0	0.6	−1.70	46
58.6248	0.34970	4 2 2 — 5 1 5	5 — 5	4 — 5	−1.1	−0.7	−1.66	79
60.0128	0.08870	3 2 2 — 4 1 3	2 — 4	−2 — −2	5.2	−2.7	1.92	52
60.0128	0.10810	3 2 2 — 4 1 3	2 — 4	−1 — −1	4.4	−3.1	1.42	123
60.0128	0.13080	3 2 2 — 4 1 3	2 — 4	0 — 0	1.0	−0.9	1.06	179
60.0128	0.13450	3 2 2 — 4 1 3	4 — 4	4 — 4	4.7	−2.8	1.68	41
60.0128	0.14990	3 2 2 — 4 1 3	3 — 4	3 — 3	−3.8	3.2	1.18	118
60.0128	0.15050	3 2 2 — 4 1 3	2 — 4	1 — 1	−2.5	2.9	0.89	199
60.0128	0.15690	3 2 2 — 4 1 3	2 — 4	2 — 2	1.0	−1.1	0.93	177
60.0128	0.20050	3 2 2 — 4 1 3	4 — 5	−2 — −2	−7.3	−2.3	−3.22	7
60.0128	0.21660	3 2 2 — 4 1 3	4 — 5	1 — 1	−18.2	−6.7	−2.73	16
60.0128	0.07670	3 2 2 — 4 1 3	2 — 4	−2 — −3	13.9	−5.5	2.50	116
60.0128	0.09310	3 2 2 — 4 1 3	2 — 4	−1 — −2	8.3	−4.4	1.87	164
60.0128	0.11430	3 2 2 — 4 1 3	2 — 4	0 — −1	2.7	−2.0	1.35	158
60.0128	0.13090	3 2 2 — 4 1 3	3 — 4	3 — 4	3.2	−1.9	1.69	134
60.0128	0.13850	3 2 2 — 4 1 3	2 — 4	1 — 0	1.6	−1.6	1.00	121
60.0128	0.14140	3 2 2 — 4 1 3	2 — 4	0 — 1	1.2	−1.3	0.95	74
60.0128	0.14460	3 2 2 — 4 1 3	2 — 4	2 — 3	−8.8	7.2	1.21	151
60.0128	0.14900	3 2 2 — 4 1 3	2 — 4	1 — 2	2.0	−2.1	0.98	118
60.0128	0.15860	3 2 2 — 4 1 3	2 — 4	2 — 1	1.8	−2.2	0.84	75
69.3876	0.16169	2 2 1 — 3 1 2	1 — 4	0 — 0	−10.4	8.4	1.24	35
69.3876	0.37702	2 2 1 — 3 1 2	3 — 2	−1 — −1	0.3	−0.1	2.68	35
69.3876	0.38600	2 2 1 — 3 1 2	3 — 4	2 — 2	−0.2	0.1	2.48	55
69.3876	0.50878	2 2 1 — 3 1 2	3 — 2	−2 — −2	3.3	−1.4	2.35	57
69.3876	0.03868	2 2 1 — 3 1 2	1 — 2	1 — 0	−9.7	−12.0	−0.81	74
69.3876	0.12430	2 2 1 — 3 1 2	1 — 2	1 — 0	−9.5	10.4	0.91	68
69.3876	0.16459	5 1 5 — 4 0 4	5 — 5	5 — 5	−0.4	−0.2	−1.84	386
69.3876	0.52266	5 1 5 — 4 0 4	5 — 4	−4 — −4	−17.7	7.2	2.46	163
91.8968	0.14160	4 2 2 — 4 1 3	4 — 4	−4 — −3	−1.6	−1.5	−1.05	1133
91.8968	0.20670	4 2 2 — 4 1 3	5 — 4	5 — 4	−1.7	1.3	1.27	1148
91.8968	0.22830	4 2 2 — 4 1 3	3 — 5	0 — 1	4.1	1.6	−2.55	309
91.8968	0.25540	4 2 2 — 4 1 3	3 — 5	−1 — 0	3.7	1.4	−2.60	272
92.9906	0.23486	2 2 0 — 2 1 1	2 — 2	−1 — −1	3.5	0.8	−4.54	729
92.9906	0.21504	2 2 0 — 2 1 1	2 — 2	−1 — 0	3.7	0.8	−4.58	1167
92.9906	0.22150	2 2 0 — 2 1 1	2 — 2	0 — 1	2.8	0.6	−4.51	1453
92.9906	0.23650	2 2 0 — 2 1 1	2 — 2	−2 — −1	1.8	0.4	−4.30	405
92.9906	0.24796	2 2 0 — 2 1 1	2 — 2	0 — −1	3.1	0.7	−4.51	976
92.9906	0.25877	2 2 0 — 2 1 1	2 — 2	1 — 0	3.2	0.8	−4.22	1114
92.9906	0.26065	2 2 0 — 2 1 1	2 — 2	1 — 2	3.1	0.8	−4.15	1098
92.9906	0.38674	2 2 0 — 2 1 1	2 — 2	2 — 1	4.9	2.0	−2.49	661
92.9906	0.43284	2 2 0 — 2 1 1	2 — 2	−1 — −2	3.3	1.3	−2.45	373
92.9906	0.47371	2 2 0 — 2 1 1	2 — 3	2 — 3	2.9	1.1	−2.62	243
92.9906	0.02708	3 2 1 — 3 1 2	3 — 4	−3 — −3	3.7	−0.3	2.17	1459
92.9906	0.03854	3 2 1 — 3 1 2	3 — 4	−2 — −2	1.9	−0.8	1.58	1524
92.9906	0.04840	3 2 1 — 3 1 2	4 — 4	3 — 3	3.3	1.7	−2.23	411
92.9906	0.05635	3 2 1 — 3 1 2	3 — 4	−1 — −1	−0.5	0.3	1.94	682
92.9906	0.07046	3 2 1 — 3 1 2	3 — 4	−2 — −2	2.3	1.3	−1.39	1553
92.9906	0.07558	3 2 1 — 3 1 2	3 — 4	3 — 3	2.3	0.8	1.06	2254
92.9906	0.08892	3 2 1 — 3 1 2	4 — 4	1 — 1	1.3	0.7	−1.14	2583
92.9906	0.23809	3 2 1 — 3 1 2	2 — 4	−1 — −1	1.6	1.3	−0.15	930
92.9906	0.24010	3 2 1 — 3 1 2	4 — 5	1 — 2	3.4	19.7	−0.17	3670
92.9906	0.01397	3 2 1 — 3 1 2	2 — 4	1 — 0	−1.6	0.7	2.46	187
92.9906	0.01574	3 2 1 — 3 1 2	2 — 4	0 — 1	2.7	−0.4	1.80	601
92.9906	0.02726	3 2 1 — 3 1 2	2 — 4	2 — 1	−0.1	0.1	2.20	1003
92.9906	0.03037	3 2 1 — 3 1 2	4 — 3	−2 — −1	1.8	0.5	−3.38	786
92.9906	0.03478	3 2 1 — 3 1 2	3 — 4	−3 — −2	3.2	−2.0	1.61	1330
92.9906	0.03479	3 2 1 — 3 1 2	2 — 4	1 — 2	−0.6	0.3	1.54	1850
92.9906	0.03867	3 2 1 — 3 1 2	3 — 4	−3 — −2	0.5	−0.3	1.55	1037
92.9906	0.04429	3 2 1 — 3 1 2	3 — 4	3 — 2	0.4	−0.3	1.70	1929
92.9906	0.04506	3 2 1 — 3 1 2	4 — 3	−1 — 0	1.3	0.6	−2.28	1795
92.9906	0.05223	3 2 1 — 3 1 2	4 — 3	1 — 0	1.6	0.7	−2.19	1506

TABLE II (*Continued*)

Laser line (cm^{-1})[a]	Resonant field (T)[c]	Assignment[b] $N_{K_aK_c}$	J	M_J	Obs.−Calc. (MHz)	(G)[c]	TR[d]	Int[e]
92.9906	0.05731	3 2 1 — 3 1 2	3 — 4	0 — −1	−0.4	0.4	0.94	3232
92.9906	0.06174	3 2 1 — 3 1 2	3 — 4	−2 — −1	0.4	−0.5	0.90	2994
92.9906	0.06780	3 2 1 — 3 1 2	3 — 4	−3 — −2	3.6	2.6	−1.39	1527
92.9906	0.07220	3 2 1 — 3 1 2	2 — 4	2 — 3	0.4	−0.4	1.04	2892
92.9906	0.07220	3 2 1 — 3 1 2	3 — 4	−1 — −2	−1.5	−1.1	−1.38	2152
92.9906	0.08129	3 2 1 — 3 1 2	4 — 2	0 — 1	1.7	1.4	−1.19	2915
92.9906	0.08362	3 2 1 — 3 1 2	4 — 4	4 — 3	0.4	−0.4	1.12	1843
92.9906	0.09803	3 2 1 — 3 1 2	4 — 2	2 — 1	0.6	0.6	−1.09	1891
92.9906	0.16577	3 2 1 — 3 1 2	3 — 4	−1 — 0	2.6	−12.1	0.22	5488
92.9906	0.16577	3 2 1 — 3 1 2	3 — 4	1 — 0	−2.0	9.2	0.21	5471
92.9906	0.21821	3 2 1 — 3 1 2	3 — 4	−2 — −1	1.5	8.8	−0.17	4724
92.9906	0.24266	3 2 1 — 3 1 2	3 — 4	0 — −1	0.5	3.2	−0.15	5717
92.9906	0.28690	3 2 1 — 3 1 2	4 — 2	1 — 2	2.1	9.7	−0.21	2811
96.6363	0.33980	3 2 2 — 3 1 3	2 — 2	−1 — −1	−5.4	1.0	5.29	255
96.6363	0.56940	3 2 2 — 3 1 3	3 — 2	2 — 2	−1.0	0.4	2.69	183
96.6363	0.63970	3 2 2 — 3 1 3	3 — 4	−3 — −3	−2.1	0.8	2.73	294
96.6363	0.64370	3 2 2 — 3 1 3	2 — 4	−2 — −2	−3.9	1.5	2.70	642
96.6363	0.79730	3 2 2 — 3 1 3	3 — 4	3 — 3	−6.9	2.6	2.69	196
96.6363	0.30330	3 2 2 — 3 1 3	2 — 2	0 — 1	−11.4	2.2	5.14	322
96.6363	0.32880	3 2 2 — 3 1 3	2 — 2	−1 — 0	−6.2	1.2	5.17	423
96.6363	0.33200	3 2 2 — 3 1 3	2 — 2	1 — 0	−8.8	1.7	5.18	495
96.6363	0.56150	3 2 2 — 3 1 3	2 — 4	0 — −1	−2.2	0.8	2.74	171
96.6363	0.56880	3 2 2 — 3 1 3	3 — 2	1 — 2	−3.5	1.3	2.69	209
96.6363	0.63860	3 2 2 — 3 1 3	3 — 2	0 — 1	−0.8	0.3	2.66	197
96.6363	0.17930	4 2 3 — 4 1 4	3 — 4	3 — 3	−3.7	−0.9	−4.28	253
96.6363	0.18880	4 2 3 — 4 1 4	3 — 4	2 — 2	1.6	0.4	−4.44	354
96.6363	0.20020	4 2 3 — 4 1 4	3 — 4	1 — 1	13.1	2.9	−4.56	326
96.6363	0.21040	4 2 3 — 4 1 4	3 — 4	0 — 0	−3.4	−0.7	−4.62	208
96.6363	0.48980	4 2 3 — 4 1 4	5 — 4	3 — 3	−1.9	−0.8	−2.46	273
96.6363	0.48980	4 2 3 — 4 1 4	3 — 5	3 — 3	−7.6	−2.6	−2.96	103
96.6363	0.60100	4 2 3 — 4 1 4	5 — 4	−3 — −3	6.7	2.7	−2.50	133
96.6363	0.60560	4 2 3 — 4 1 4	5 — 4	4 — 4	1.7	0.7	−2.48	565
96.6363	0.18860	4 2 3 — 4 1 4	3 — 4	3 — 4	−4.0	−1.0	−3.92	130
96.6363	0.18860	4 2 3 — 4 1 4	3 — 4	2 — 1	8.2	1.8	−4.52	162
96.6363	0.20320	4 2 3 — 4 1 4	3 — 4	1 — 0	9.3	2.0	−4.56	263
96.6363	0.20740	4 2 3 — 4 1 4	3 — 4	0 — 1	0.1	0.0	−4.63	138
96.6363	0.21140	4 2 3 — 4 1 4	3 — 4	−1 — 0	0.7	0.2	−4.63	277
96.6363	0.21300	4 2 3 — 4 1 4	3 — 4	−2 — −1	−2.0	−0.4	−4.51	336
96.6363	0.21590	4 2 3 — 4 1 4	3 — 4	−3 — −2	0.1	0.0	−4.31	318
96.6363	0.21760	4 2 3 — 4 1 4	3 — 4	0 — −1	−2.0	−0.4	−4.55	298
96.6363	0.22570	4 2 3 — 4 1 4	5 — 4	−4 — −3	2.8	0.7	−3.97	260
96.6363	0.23160	4 2 3 — 4 1 4	3 — 4	−1 — −2	2.4	0.6	−4.40	233
96.6363	0.27370	4 2 3 — 4 1 4	5 — 4	−5 — −4	−3.1	−1.2	−2.61	194
96.6363	0.44560	4 2 3 — 4 1 4	5 — 4	2 — 3	0.9	0.4	−2.43	201
96.6363	0.45080	4 2 3 — 4 1 4	5 — 4	−1 — −2	−0.8	−0.3	−2.41	258
96.6363	0.55080	4 2 3 — 4 1 4	5 — 4	−2 — −3	1.7	0.7	−2.43	297
96.6363	0.67270	4 2 3 — 4 1 4	4 — 4	−4 — −3	−0.2	−0.1	−2.59	181
117.2095	0.09320	3 2 2 — 2 1 1	4 — 2	1 — 1	5.3	1.1	−4.82	1543
117.2095	0.09610	3 2 2 — 2 1 1	4 — 2	0 — 0	6.5	1.4	−4.77	2955
117.2095	0.10630	3 2 2 — 2 1 1	4 — 2	−1 — −1	0.1	0.0	−4.43	2839
117.2095	0.16000	3 2 2 — 2 1 1	4 — 2	−2 — −2	−1.8	−0.7	−2.54	1578
117.2095	0.21000	3 2 2 — 2 1 1	3 — 2	2 — 2	−4.3	−1.8	−2.41	1486
117.2095	0.24620	3 2 2 — 2 1 1	3 — 2	−1 — −1	0.5	0.2	−2.47	1357
117.2095	0.09510	3 2 2 — 2 1 1	4 — 2	2 — 1	1.6	0.3	−4.84	4123
117.2095	0.09770	3 2 2 — 2 1 1	4 — 2	1 — 0	−2.2	−0.5	−4.78	3583
117.2095	0.10470	3 2 2 — 2 1 1	4 — 2	−2 — −1	−1.5	−0.3	−4.41	1911
117.2095	0.10800	3 2 2 — 2 1 1	4 — 2	0 — −1	−1.2	−0.3	−4.45	1872
117.2095	0.15760	3 2 2 — 2 1 1	4 — 2	−3 — −2	1.0	0.4	−2.54	1973
117.2095	0.20864	3 2 2 — 2 1 1	4 — 2	3 — 2	−3.0	−1.2	−2.41	4998
117.2095	0.24527	3 2 2 — 2 1 1	3 — 2	−2 — −1	−3.2	−1.3	−2.46	1744
117.2095	0.28714	3 2 2 — 2 1 1	4 — 3	2 — 1	−4.5	−1.6	−2.77	1396

[a] See Table I.

[b] The assignment given for J is that with which the given M_J level correlates at zero field.

[c] 1 T ≡ 10^4 G.

[d] Calculated tuning rate in MHz/G.

[e] Calculated relative line intensity, including Boltzmann factor for 300 K.

TABLE III. Molecular parameters for the ground $\tilde{X}\,^3B_1$ state of CD_2 (in cm^{-1}).[a]

Rotation	A	37.786 863(62)[b]
	$\frac{1}{2}(B+C)$	3.962 178(16)
	$\frac{1}{2}(B-C)$	0.267 47(10)
Centrifugal distortion	Δ_K	0.560 215(17)
	Δ_{NK}	$-0.496\,40(98)\times10^{-2}$
	Δ_N	$0.929\,5(71)\times10^{-4}$
	δ_K	$0.272\,8(54)\times10^{-2}$
	δ_N	$0.226\,4(28)\times10^{-4}$
	Φ_K	0.019 6[c]
	Φ_{KN}	$-0.243\,7(19)\times10^{-3}$
	Φ_{NK}	$-0.143(30)\times10^{-5}$
Spin–spin	D	0.776 484(96)
	E	0.040 592(66)
Spin–rotation	ϵ_{aa}	$0.028\,6(37)\times10^{-2}$
	ϵ_{bb}	$-0.260\,7(15)\times10^{-2}$
	ϵ_{cc}	$-0.207\,7(24)\times10^{-2}$

[a]Parameters not included here were fixed at zero, except for g factors fixed at theoretically estimated values (see the text).
[b]The numbers in parentheses are one standard error from the least-squares fit in units of the last quoted digit.
[c]Fixed at the value obtained from a fit to nonrigid bender (Ref. 7) energy levels.

TABLE IV. Comparison of spin–spin interaction parameters of isotopic forms of CH_2 for the vibronic ground state (in cm^{-1}).

	D	E
$^{13}CD_2$ (this work)	0.7765(1)	0.040 59(7)
$^{12}CD_2$ (Ref. 2)	0.7784(1)	0.039 91(4)
$^{13}CH_2$ (Ref. 5)	0.7801(13)	0.041 76(53)

TABLE VI. Parameters for the (100) excited vibrational state of $CH_2(\tilde{X}\,^3B_1)$ (in cm^{-1}).[a]

Parameter[b]	Value
A	69.000 31(20)
B	8.281 18(20)
C	7.102 02(9)
D	0.785 44(88)
E	0.042 02(38)
ϵ_{aa}	0.002 1(7)
ϵ_{bb}	−0.003 79(27)
ϵ_{cc}	−0.003 61(26)

[a]From a fit to the data of Table V of this paper and Table V of Sears *et al.* (Ref. 2). Because of the limited number of observed rotational transitions and the possibility of perturbations in this vibrational state, the precise values of these parameters are not very meaningful.
[b]All the centrifugal distortion parameters were fixed at their ground state values [see Table III of Sears *et al.* (Ref. 2)].

makes it difficult to conduct a systematic search. For example, the Q-branch transitions 3_3-3_2, 4_3-4_2, etc., should occur[7] at approximately 146 cm^{-1}. Although some LMR signals were obtained using a laser line at 141.8 cm^{-1}, they could not be assigned to rotational transitions in CD_2.

Although not part of our study of CD_2 we have, since publishing Ref. 2, found some resonances due to the rotational transitions $1_{10}-1_{01}$ and $2_{12}-1_{01}$ for CH_2 in the ν_1 excited vibrational state, and it is convenient to report them here. The positions of these resonances are given in Table V. Previously we detected resonances due to the transitions $2_{11}-2_{02}$ and $3_{12}-3_{03}$ for CH_2 in the ν_1 state (see Table V of Ref. 2). Combining this data

TABLE V. New observed transitions in the (100) excited vibrational state of CH_2.[a]

Laser line (cm^{-1})	Resonant field (T)	Assignment $N_{K_aK_c}$	J	M	Obs.–Calc. (MHz)
60.012 827[c]	0.027 84[c]	$1_{10}-1_{01}$	2 — 2	−2 — −1	−5
	0.028 94		2 — 2	1 — 2	−5
	0.031 29		2 — 2	0 — 1	−8
	0.031 29		2 — 2	−1 — 0	−3
	0.292 96		2 — 2	−1 — 0	−6
	0.519 14		1 — 2	1 — 0	0
	0.921 60		1 — 0	−1 — 0	−11
88.863 420[d]	0.236 31	$2_{12}-1_{01}$	2 — 2	−1 — −1	−14
	0.298 56		2 — 2	−2 — −2	−26
	0.469 24		2 — 2	1 — 1	−10
	0.599 54		3 — 2	−1 — −1	+36
	0.646 22		2 — 1	−1 — −1	−5
	0.135 86		3 — 0	−1 — 0	+32
	0.211 73		2 — 2	0 — −1	−15
	0.289 95		2 — 2	1 — 0	−15
	0.343 05		2 — 2	−1 — 0	−2
	0.414 86		2 — 2	−2 — −1	−28
	0.486 97		2 — 2	0 — 1	−12
	0.491 77		2 — 2	2 — 1	+14
	0.634 82		3 — 2	0 — −1	+46

[a]See also Table V of Sears *et al.* (Ref. 2).
[b]118.6 μm laser line of CH_2F_2.
[c]1 T = 10^4 G.
[d]112.5 μm laser line of CH_2DOH.

for ν_1 state CH_2 we determine the effective Hamiltonian parameters given in Table VI.

B. Using the semirigid bender Hamiltonian

As with CH_2 it is of interest to fit the rotation bending transition wave numbers of CD_2 using the semirigid bender Hamiltonian.[10] The data for the fit are obtained from the results of this paper and of the following paper[5] on the ν_2 band of CD_2, after suppressing the fine structure; they are summarized in Table VII. The semirigid bender Hamiltonian treats the molecule as rotating and bending within an effective bending potential function with bond lengths that are allowed to vary with the bending angle. The effective bending potential function and the bond length function will vary with isotopic substitution and with excitation of the stretching vibrations ν_1 and ν_3 because of the effects of the averaging over the stretching vibrations.

By adjusting two parameters in the effective bending function V and two in the bond length function R, in the semirigid bender Hamiltonian, the least squares fit of the data in Table VII is obtained with

$$V/\mathrm{cm}^{-1} = -6943.0(3.5)\rho^2 + 7514.4(3.1)\rho^4 - 2698\rho^6 + 500\,\rho^8 \quad (1)$$

and

TABLE VII. Experimentally derived zero-field rotation and rotation-vibration transitions in $CD_2(\tilde{X}\,^3B_1)$ with fine structure splittings removed (in cm^{-1}).

$N_{K_aK_c}$	Observed	Obs.−Calc.[c]
(0, 0, 0) state[a]		
$1_{11}-2_{02}$	17.1920	−0.0251
$1_{10}-1_{01}$	33.5554	−0.0009
$2_{11}-2_{02}$	34.1038	0.0046
$3_{12}-3_{03}$	34.9365	0.0125
$1_{11}-0_{00}$	40.9556	−0.0002
$2_{12}-1_{01}$	48.3728	−0.0034
$3_{13}-2_{02}$	55.5373	−0.0141
$4_{22}-5_{15}$	58.9443	0.0451
$3_{22}-4_{13}$	60.1329	−0.0407
$2_{21}-3_{12}$	69.0165	−0.0163
$5_{13}-4_{04}$	69.1423	−0.0601
$4_{22}-4_{13}$	92.0210	−0.0376
$3_{21}-3_{12}$	92.8054	−0.0106
$2_{20}-2_{11}$	93.5938	0.0114
$3_{22}-3_{13}$	96.0123	0.0364
$4_{23}-4_{14}$	97.1516	0.0808
$3_{22}-2_{11}$	117.4458	0.0177
ν_2 band[c]		
$3_{03}-3_{12}$	717.0699	0.0286
$4_{04}-4_{13}$	715.7102	0.0184
$5_{05}-5_{14}$	713.9986	0.0036
$6_{06}-6_{15}$	711.9297	−0.0153
$7_{07}-7_{16}$	709.4992	−0.0359

[a] From the present results.
[b] From McKellar *et al.* (Ref. 6).
[c] Calculated using the semirigid bender Hamiltonian (Ref. 10) with the V and R_{CD} functions as given in Eqs. (1) and (2).

TABLE VIII. Predicted CHD rotation bending energies in several (v_1, v_2, v_3) states using the semirigid bender Hamiltonia (in cm^{-1}).

N	K_a	K_c	(0, 0, 0)	(0, 1, 0)	(0, 2, 0)
0	0	0	0.00	867.16	1623.23
1	0	1	10.70	877.91	1634.05
	1	1	59.14	982.84	1890.40
	1	0	59.89	983.77	1891.52
2	0	2	32.11	899.41	1655.67
	1	2	79.77	1002.32	1910.84
	1	1	82.02	1006.10	1914.21
	2	1	214.55	1212.25	2227.12
	2	0	214.56	1212.25	2227.14
3	0	3	64.18	931.65	1688.12
	1	3	110.71	1034.04	1941.52
	1	2	115.21	1039.60	1948.24
	2	2	246.61	1244.39	2259.45
	2	1	246.65	1244.39	2259.53
	3	1	448.17	1516.08	2614.08
	3	0	448.17	1516.08	2614.08

$$R_{CD}/\text{Å} = 1.073\,95(92) + 0.0207(20)\rho^4\,, \quad (2)$$

where ρ is the supplement of the bond angle in radians, the numbers in parentheses are one standard error of the varied coefficients, and the coefficients of ρ^6 and ρ^8 in V were held fixed at the values[3] for CH_2. The standard deviation of the fit to the 22 transitions is 0.030 cm^{-1} and the (observed-calculated) values are given in Table VII. In this effective potential the equilibrium angle is 133.6° and the barrier to linearity is 1989.9 cm^{-1}.

We can use the results of this fit together with the results of the semirigid bender fit to the CH_2 data[3] to predict the rotation-bending energy levels of CHD. To a good approximation the effective bending function in CHD will be the average of those for CH_2 and CD_2, i.e., for CHD we have

$$V = -6989\rho^2 + 7536\rho^4 - 2698\rho^6 + 500\rho^8\,. \quad (3)$$

For CHD we can take the CH bond length function to be the same as in CH_2,[3] i.e.,

$$R_{CH} = 1.0740 - 0.0239\rho^4\,, \quad (4)$$

and the CD bond length function to be the same as in CD_2. Using Eqs. (2), (3), and (4) in the semirigid bender Hamiltonian yields the CHD rotation-bending term values given in Table VIII.

These predictions for CHD, although not as precise as would be obtained using the nonrigid bender Hamiltonian, are nonetheless sufficiently precise to aid the experimental search for CHD spectra. The diagonalization of the nonrigid bender Hamiltonian for an unsymmetrical molecule (such as CHD) has yet to be computer programmed.

IV. SUMMARY AND DISCUSSION

We have reported here the detection and assignment of seventeen rotational transitions in the ground vibronic state of the CD_2 radical. Analysis of the spectra yields

TABLE IX. Calculated energy levels for the ground vibronic state of CD_2 (in cm^{-1}).[a]

	F_1[b]	F_2	F_3
0_{00}	−0.005 70	...	...
1_{01}	7.866 21	8.185 14	7.411 01
1_{11}	40.972 06	40.837 54	41.175 59
1_{10}	41.503 81	41.321 81	41.781 16
2_{02}	23.682 16	24.025 01	23.517 13
2_{12}	56.247 45	56.447 84	56.161 48
2_{11}	57.829 00	57.978 40	57.774 10
2_{21}	151.524 52	151.191 24	151.715 57
2_{20}	151.530 78	151.197 12	151.722 05
3_{03}	47.406 35	47.763 88	47.307 32
3_{13}	79.221 09	79.517 23	79.141 68
3_{12}	82.371 46	82.614 78	82.313 22
3_{22}	175.306 06	175.314 02	175.324 45
3_{21}	175.337 09	175.344 06	175.355 85
4_{04}	79.008 81	79.376 96	78.942 95
4_{14}	109.860 73	110.200 87	109.799 83
4_{13}	115.096 32	115.382 61	115.052 29
4_{23}	207.062 32	207.214 69	207.048 17
4_{22}	207.154 68	207.305 27	207.141 10
5_{05}	118.455 00	118.831 67	118.410 54
5_{15}	148.147 34	148.512 73	148.102 81
5_{14}	155.980 08	156.291 01	155.950 10
5_{24}	246.759 70	246.988 62	246.742 14
5_{23}	246.973 68	247.199 81	246.956 89

[a]Calculated using the parameters of Table III. The energies are not reliable to the quoted precision of 0.000 01 cm^{-1}, but differences corresponding to observed transitions (see Table I) should approach this accuracy.

[b]Fine structure levels are labeled according to F_1 for $J=N+1$, F_2 for $J=N$, and F_3 for $J=N-1$. The 0_{00} energy level is shifted slightly from zero by spin–spin interaction with the F_3 component of 2_{02}.

very precise values for the major molecular parameters appearing in the effective rotational Hamiltonian for the state. A fit to the data obtained here and in Ref. 6 using the semirigid bender Hamiltonian has also been made and this has allowed us to predict the rotation-bending energy levels for CHD.

The electronic spin–spin parameters obtained from the effective Hamiltonian fit can be compared to those estimated from ESR experiments in low temperature matrices.[11–13] In such experiments the major parameter D was determined to be 0.76 cm^{-1} with an error dominated by the perturbing effects of the matrix; this error is not very precisely known but the present result is within the expected uncertainty. The parameter E represents the anisotropic part of the spin–spin interaction and it is not well determined in the ESR experiments because of averaging effects due to the nearly free rotation of the molecule about its a axis in the matrix. The observed difference between D for CH_2 and for CD_2 (see Table IV) is an order of magnitude larger than calculated by Langhoff and Kern,[13] whereas the change in E is a factor of 2 larger. We are not aware of any *ab initio* calculation of D or E for $^{13}CH_2$.

In Table IX we give the energies of some of the lowest rotational levels of the CD_2 radical calculated using the parameters given in Table III. In CH_2 the proximity of the levels 4_{04} and 3_{13}, which are connected by an allowed electric dipole transition, permitted the observation of the transition by traditional microwave techniques.[14] In CD_2 a much closer coincidence occurs between the 3_{13} and 4_{04} levels. The frequencies of the strongest fine structure components of the $3_{13}-4_{04}$ transition are predicted to lie at around 5 GHz which is inconveniently low for conventional microwave spectroscopy. The transitions $2_{12}-3_{03}$ and $5_{05}-4_{14}$ are predicted to lie around 260 GHz in a suitable region for conventional millimeter-wave spectroscopy. They are inconveniently low for the far infrared LMR technique used in the present work.

ACKNOWLEDGMENTS

We are grateful to Murray Bush and Per Jensen for help in some of the programming, and we also thank J. M. Brown and A. O'Keefe for assistance in taking some of the spectra.

[1]T. J. Sears, P. R. Bunker, and A. R. W. McKellar, J. Chem. Phys. 75, 4731 (1981).
[2]T. J. Sears, P. R. Bunker, A. R. W. McKellar, K. M. Evenson, D. A. Jennings, and J. M. Brown, J. Chem. Phys. 77, 5348 (1982).
[3]T. J. Sears, P. R. Bunker, and A. R. W. McKellar, J. Chem. Phys. 77, 5363 (1982).
[4]P. Jensen, P. R. Bunker, and A. R. Hoy, J. Chem. Phys. 77, 5370 (1982).
[5]A. R. W. McKellar and T. J. Sears, Can. J. Phys. 61, 480 (1983).
[6]A. R. W. McKellar, C. Yamada, and E. Hirota, J. Chem. Phys. 79, 1220 (1983).
[7]P. R. Bunker and P. Jensen, J. Chem. Phys. 79, 1224 (1983).
[8]C. E. Barnes, J. M. Brown, A. Carrington, J. Pinkstone, T. J. Sears, and P. J. Thistlethwaite, J. Mol. Spectrosc. 72, 86 (1978).
[9]R. F. Curl, Mol. Phys. 9, 585 (1965).
[10]P. R. Bunker and E. M. Landsberg, J. Mol. Spectrosc. 67, 374 (1977).
[11]B. R. Bicknell, W. R. M. Graham, and W. Weltner, Jr., J. Chem. Phys. 64, 3319 (1976).
[12]R. A. Bernheim, T. Adl, H. W. Bernard, A. Bongeo, P. S. Wang, R. Wang, L. S. Wood, and F. S. Skell, J. Chem. Phys. 64, 2747 (1976).
[13]E. Wasserman, V. J. Kuck, R. S. Hutton, E. D. Anderson, and W. A. Yager, J. Chem. Phys. 54, 4120 (1971).
[14]F. J. Lovas, R. D. Suenram, and K. M. Evenson, Astrophys. J. Lett. 207, L181 (1968).
[15]S. R. Langhoff and C. W. Kern, *Applications of Electronic Structure Theory*, in *Modern Theoretical Chemistry*, edited by H. F. Schaefer III (Plenum, New York, 1977), Vol. IV.